Polymer Degradation and Stability 218 (2023) 110571

Contents lists available at ScienceDirect

Polymer Degradation and Stability

journal homepage: www.journals.elsevier.com/polymer-degradation-and-stability

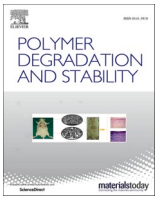

Development of non-combustible weaveable yarn through oxidative control of a textile acrylic fibre

Esfandiar Pakdel [a,b], Masihullah Jabarulla Khan [a], Nguyen Le Thao Nguyen [a], Maxime Maghe [a], Russell J. Varley [a,*]

[a] Carbon Nexus at the Institute for Frontier Materials, Deakin University, Geelong, VIC 3216, Australia
[b] JC STEM Lab of Sustainable Fibers and Textiles, School of Fashion and Textiles, The Hong Kong Polytechnic University, Hung Hom, Kowloon, Hong Kong

ARTICLE INFO

Keywords:
Fire-retardant textiles
Acrylic fibre and yarn
PAN oxidation
Stabilisation

ABSTRACT

Acrylic fibre is considered to be artificial wool in the textile industry, but in contrast with natural wool, it vigorously burns producing black smoke and toxic gases. This not only has hindered its technical applications, but also poses safety risks to the end-users of acrylic-based products. This research aims at enhancing the fire-retardancy of acrylic yarns using a facile thermal stabilisation process which is based on controlling the oxidation temperature and residence period. To this end, acrylic yarns are thermally processed according to six different time and temperature profiles ranging from 220 to 280 °C, with residence periods ranging from 22 to 28 min. The oxidised yarns were characterised using FTIR, DSC, and TGA techniques and the effects of the oxidative thermal treatment on physical characterises, and surface morphology of yarns and fibres were discussed. The results showed that the acrylic yarn undergone the oxidation process based on 240–255–270–280 °C heating profile for 28 min at each step had a sufficiently high degree of cyclisation with an excellent fire retardancy. Furthermore, the stabilised acrylic yarn was strong enough to be woven into a plain weave fabric using a laboratory scale loom while displaying non-combustible behaviour during cyclic exposure to flame. These results present a novel pathway for the development of a low cost, non-combustible fabric ideally suited for applications in extreme environments.

1. Introduction

Acrylic fibre is made from a polyacrylonitrile polymer containing at least 85 % by weight of acrylonitrile monomer, ($CH_2CH(C{\equiv}N)$), and is the third most important conventional synthetic fibre after polyester and polyamide [1,2]. Often referred to as artificial wool, acrylic fibers are valued for their warmth, softness, bulkiness, high elasticity and resistance to moths and mildew. This has led to their use in a wide variety of home textile products including clothing, carpets, curtain, upholstery, footwears, and blankets, amongst others [2–4]. However, compared with other types of fibres such as cotton and viscose, acrylic is one of the most flammable fibres, highlighted by very low limiting oxygen index (LOI) measurements of around 18 % [5,6]. During heating, acrylic fibres shrink readily, exhibiting vigorous burning behaviour after ignition and often generating toxic gases [7,8].

To address this deficiency, acrylic fibres are often mixed with wool to enhance their inherent fire retardancy. Other approaches include modifying the acrylic polymer chain through copolymerisation, adding fire retardants to the spinning dope, or surface finishing [3,8,9]. To modify the polymeric chain, some comonomers such as vinylidene chloride have been used in developing commercial modacrylics with improved fire resistance. However, these additives are mostly halogenated and contain phosphorous compounds which are not environmentally friendly and can generate smog and toxic gases during the burning process [6]. Adding additives to spinning dopes shows effectiveness only in high concentrations, which can cause some defects in the structures of spun fibres by reducing their integrity and mechanical characteristics [6]. Similarly, to achieve an effective surface finishing, organic or inorganic flame retreatant ingredients are required in high contents which can hamper the durability, flexibility, and applicability of the developed products [10,11]. Moreover, the detachment of fire-retardant agents such as different types of nanomaterials during the products preparation, handling and use, can pose serious health risk to human health and environment. These drawbacks highlight the

* Corresponding author.
E-mail address: russell.varley@deakin.edu.au (R.J. Varley).

https://doi.org/10.1016/j.polymdegradstab.2023.110571
Received 16 August 2023; Received in revised form 2 October 2023; Accepted 18 October 2023
Available online 20 October 2023

Table 1
Stabilisation profiles used to produce fire-retardant acrylic yarns.

Samples	Air Speed	Stage 1		Stage 2		Stage 3		Stage 4	
	m/s	Temp (°C)	Time (Min)	Temp (°C)	Time (Min)	Temp (°C)	Time (Min)	Temp (°C)	Time (Min)
S1	4	220	28	240	28	250	28	265	28
S2	4	230	28	245	28	260	28	270	28
S3	4	235	28	250	28	265	28	275	28
S4	4	240	22	255	22	270	22	280	22
S5	4	240	25	255	25	270	25	280	25
S6	4	240	28	255	28	270	28	280	28

necessity of developing more practical and effective methods for improving the fire retardancy of acrylic fibres.

Numerous studies have been reported on developing flame-retardant acrylic fibres. For instance, Tsafack and Grützmacher [12] covalently attached different types of phosphorus containing monomers including diethyl (acryloyloxyethyl) phosphate (DEAEP), diethyl-2-(methacryloyloxyethyl) phosphate (DEMEP), diethyl (acryloyloxymethyl) phosphonate (DEAMP) and dimethyl (acryloyloxymethyl) phosphonate (DMAMP) onto polyacrylonitrile (PAN) fibres via a low-pressure plasma technique. The synergistic role of phosphorous compounds is related to their char forming effect which reduces the generation of volatiles, but also their radical scavenging role in the gaseous phase [12]. Similarly, Ren et al. [13] used a UV-induced graft polymerisation technique to attach hydroxyethyl methacrylate (HEMA) onto PAN fibres followed by treatment with phosphoric acid and urea which increased the LOI value to 32 %. Tsai et al. [7] reported the improved flame retardancy of acrylic and modacrylic fibres after the addition of tri (dibromo propyl) phosphate and antimony oxide, respectively, to their spinning steps. Ren et al. [14] showed the flame retardancy of polyvinyl alcohol/polyacrylonitrile (PVA/PAN) blended fibre which was spun through a wet-spinning approach. Fire retardancy was obtained via the immersion of the spun PVA/PAN fibres into a solution containing phosphorus acid (50 wt%) and 5 g urea. Metal-based flame retardants have been used as cheaper and more eco-friendly candidates for improving the properties of acrylic fibres. Xu et al. [15] investigated the effect of modification of polyacrylonitrile (PAN) fibres with hydrazine hydrate and aqueous metal acetate solution (5 % by mass). It was reported that the presence of metal ions contributed to forming cyclic structures and char residue on PAN fibres resulting in the improved flame retardancy. Zhou et al. [16] post-treated acrylic fibres with sodium ions, hydrazine hydrate and aqueous sodium hydroxide to improve the flame resistance of the fibres. It was reported that after increasing the treatment time of fibres in NaOH solution containing Na^{+}ions, the LOI level of fibres increased to around 60 from 18. Despite the improvement in the flame retardancy, some reductions in tensile strength of treated fibres were reported. Flame-retardant PAN fibres were developed using diethylenetriamine and zinc sulfate (zinc ions (Zn^{2+})) by Yan et al. [9] where the treated fibres showed LOI values up to 47. Carosio et al. [17] used a layer-by-layer coating technique using chitosan and montmorillonite clay to develop flame retardant acrylic fibres. The multilayer clay nanoplatelets were deposited and stuck together with chitosan and provided self-extinguishing behaviour and prevented melt-dripping of burning fibres.

PAN fibres are widely used as the precursor in the production of carbon fibres [18–20]. The production process of carbon fibres from PAN consists of two main steps of stabilisation and carbonisation [18,20,21]. During the stabilisation step, a ladder like structure is formed via cyclisation of the nitrile groups, while dehydrogenation and oxidation also occur in parallel [21,22]. This exothermic process takes place at the temperature ranges of 200–300 °C and the resultant oxidised fibres exhibit high fire retardancy due to the thermal stability of the hexagonal nitrogen containing carbon rings formed [23]. The oxidised PAN fibres have a far higher melting temperature than other types of conventional fibres and therefore have been used in different industries including firefighter's clothing, thermal and acoustic products, and aerospace, amongst others [23]. Ismar et al. [24] used this technique to develop non-flammable PAN nanofibre webs where PAN fibre was oxidised at 300 °C for 1 h at atmospheric pressure increasing the LOI index of the fibres to 49. Kil and Lee [21] reported flame retardant PAN fibres developed through oxidation with electron-beam irradiation and plasma-assisted thermal stabilisation over temperature profiles from 210 to 280 °C. It was found that the electron-beam irradiation reduced the cyclisation onset temperature and the plasma thermal treatment facilitated the fibres oxidation [21].

Although there are numerous research efforts towards improving the fire retardancy of PAN-based nanofibres, fibres and fabric products, enhancing the flame retardancy of the texturised acrylic yarns as a widely used textile commodity through a stepwise stabilisation process has not fully been explored. Developing an effective thermal stabilisation method for processing acrylic yarns and fibres not only can obviate the necessity of using high loadings of additives and fire-retardant agents during manufacturing steps of acrylic-based products, but it can also develop a permanent fire-retardant functionality in the processed samples. The adjustment of heating profiles for stabilising acrylic fibres and yarns is critical because if the heating is too rapid, there will be too much shrinkage, severe weight loss, and char formation on the fibres leading to a brittle fibre. Conversely, if the heating is too slow, the degree of stabilisation will be too low and the fibre will remain combustible, causing complete decomposition of the fibres at high temperatures [4]. An important aspect of the stabilised fibres which has rarely been discussed in literature is their applicability in large scale manufacturing set-ups which are common in textile industry. In this research, the suitability of the oxidised yarns for large-scale weaving process is demonstrated which in turn can facilitate the production of low-cost acrylic-based goods for advanced applications. This study, therefore, seeks to develop a new type of oxidised acrylic yarn that exhibits superior fire-retardancy while maintaining complete weavability. To do this, the effect of different parameters including stabilisation residence time and temperature on the obtained thermal, mechanical and spectroscopic characteristics are investigated.

2. Experimental

2.1. Materials and sample preparation

An 8-ply acrylic yarn was obtained from a local textile retail store. The lab-scale oxidation oven used is referred to as a Carbon Fibre simulator which is a prototype machine able to manufacture small amounts of carbon fibre in a batchwise process that provides for temperature, tension and atmospheric control. It has an oxidation oven and a carbonisation furnace (max. 1450 °C) manufactured by Furnace Engineering, Australia. The oxidation oven temperature was varied over the range of 220 to 280 °C, with the dwell time between 22 and 28 min as listed in Table 1. A sample of non-oxidised acrylic yarn was used as a control to understand the impact of oxidation on properties.

Large scale production of the oxidised acrylic yarn, sufficient for weaving into a fabric was carried out using the oxidation ovens of the continuous pilot scale carbon fibre line at Carbon Nexus, Deakin

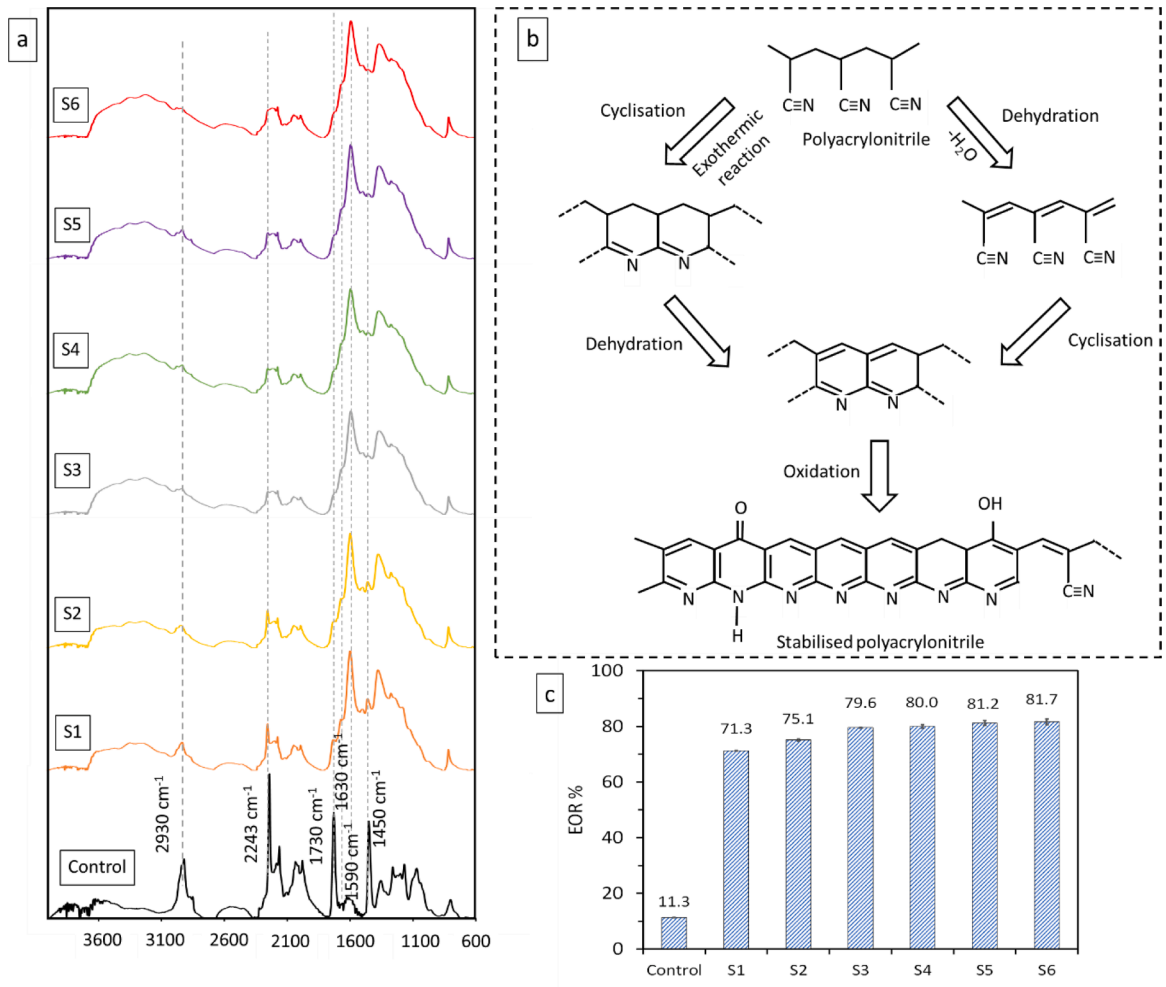

Fig. 1. (a) FTIR spectra of the control acrylic and oxidised yarns, (b) idealised reactions proposed to occur during the stabilisation process of acrylic fibres, (c) EOR (%) of the yarns subjected to the different oxidation profiles.

University. A temperature profile matching the S6 sample conditions was used while the line speed was chosen that aligned with residence times in the ovens of 28 min. To promote an even distribution of the loads applied to the yarn during processing, 10 separate yarns were oxidised simultaneously. To demonstrate similarity with the laboratory prepared fibre, DSC thermal analysis was performed which indicated similar levels of oxidation.

The warping and weaving processes of the oxidised yarns were carried out using a CCI SW550 Mini Warper, and CCI Kebalan Servo Loom, respectively. The plain weave fabric was developed based on warp and weft densities of 6 and 20 ends per inch, respectively.

2.2. Characterisation techniques

Differential scanning calorimetry (DSC) was performed using a Netzsch Polyma 214 DSC instrument from 20 °C to 400 °C with the heating rate of 10 °C/min under air atmosphere. The area underneath the exothermic peak (280–400 °C) was equivalent to the enthalpy of the reaction and was determined by the Proteus Analysis software and considered an indication of exothermic energy released during the cyclisation process. The stabilisation yield (SY%) was calculated based on the Eq. (1) from the obtained DSC curves [25] :

$$SY\% = [(\Delta H_{ox} - \Delta H_o)]/\Delta H_o \quad \times 100 \tag{1}$$

Where ΔH_{ox} and ΔH_o were the enthalpy of the oxidised and control acrylic yarns, respectively.

Scanning electron microscopy (SEM) images were taken using a Zeiss Supra 55VP (Germany). Optical microscopy images were taken using Olympus BX51M instrument. The variation of yarns diameters was measured using the ImageJ software based on the scale bar provided in the optical microscopy images. Measurements were conducted at three different spots of each yarn and the average values were reported.

Thermogravimetric analysis (TGA) and derivative thermogravimetry (DTG) curves were obtained using a TGA TA Q50 instrument under nitrogen and air atmospheres with the heating rate of 10 °C/min up to 800 °C. All data related to the residue amount, weight loss of samples, and decomposition onset temperatures were calculated using TA Universal Analysis Software.

Dynamic mechanical analysis (DMA) was used in the creep mode by applying a constant force level of 10 cN under an air atmosphere, using a Q800 DMA apparatus (TA, USA) at a heating rate of 2.5 °C.min^{-1}, from room temperature to 350 °C. Single tow samples of approximately 12 mm length were cut, then placed into the instrument. The initial length (l_o) and the yarn length after the thermal treatment was determined (l) and the yarn shrinkage was calculated by using Eq. (2).

$$Shrinkage(\%) = (l_o - l)/l_o \tag{2}$$

Fourier Transform Infrared (FTIR) spectroscopy of the samples was conducted using a Bruker Vertex 70 FTIR spectrometer (Germany) equipped with an ATR accessory over a spectral range of 600–4000 cm^{-1}. The extent of reaction (EOR) was calculated for different processed yarns based on Eq. (3) according to the data obtained from three

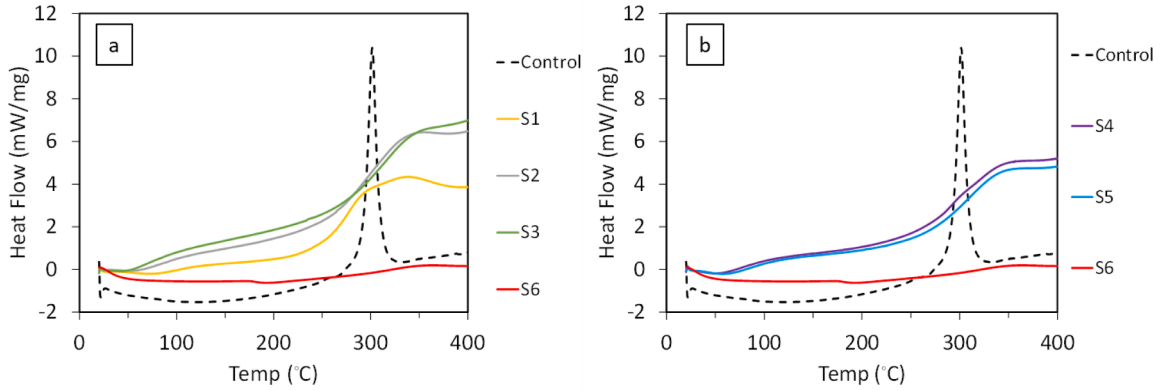

Fig. 2. DSC curves of control and oxidised yarns; illustrating the effects of (a) temperature (control, S1, S2, S3 and S6), and (b) the residence time (control, S4, S5 and S6).

specimens of each sample [25,26]. Three measurements were conducted for each sample and the average values were reported.

$$EOR\% = I(C=N)_{1590} / \left(I(C\equiv N)_{2240} + I(C=N)_{1590}\right) \quad (3)$$

Where I_{2240} and I_{1590} were the C≡N and C = N bonds peak intensity in the FTIR spectra, respectively.

The flammability of the yarns was tested by exposing the horizontally fixed yarns to gas flame for 10 s and observing the burning behaviour of the yarn. The flame retardancy of the woven fabric was further evaluated through exposing the fabric to a propane gas flame at a distance of 3 cm for 4 s over three cycles.

Stress-strain curves of pristine (control) and oxidised acrylic yarns were tested using Instron 30KN Tensile Tester based on the ASTM D2256/D2256M-10 (2015) standard test method. Three specimens from each sample were tested and the average values were reported.

3. Results and discussion

3.1. FTIR analysis

The changes in the chemical structure of yarns were monitored using FTIR spectra (Fig. 1a). During the polyacrylonitrile stabilisation process, oxygen penetrates the fibre core transforming the fibre into a cross-linked configuration [27]. Ideally this would occur prior to the oxidation of the outer layer of the fibre which can prevent further penetration of oxygen rendering the oxidation process incomplete [27]. Therefore, the heating rates, temperature, along with the residence time are all factors which need to be finely controlled. The successful production of a fire-retardant acrylic fibre depends on achieving a high degree of stabilisation and oxidation to develop ladder-like networks of hexagonal unsaturated carbon-nitrogen rings along the axis of the fibres [27,28]. This conversion occurs via three stages: cyclisation of nitrile groups, dehydrogenation and oxidation as shown in Fig. 1b. Based on the obtained FTIR spectra, the control acrylic sample showed the characteristic peaks including C—H vibrations at 1450 and 2930 cm^{-1}, and stretching vibration of nitrile (C≡N) group at 2240 cm^{-1} [29–32]. The sharp peak at 1730 cm^{-1} was related to the stretching vibration of C = O from the carboxyl group [30,33]. As a general trend, the stabilisation process reduced the intensity of peaks at 1450, 1730, 2240, 2930 cm^{-1}, and increased the intensity of peaks at 1590 and 1630 cm^{-1} and attributed to the formation of C = C and C = N bonds [34–36]. These changes suggest the initiation of the transformation of the linear structures in acrylic fibres to the ladder-like structure through cyclisation, dehydrogenation and oxidative reactions during the heat treatment process (Fig. 1b) [30,36]. Comparing the different FTIR spectra as a function of increasing temperatures, i.e., S1, S2, S3, and S6 profiles, the peak intensity at 2240 cm^{-1} decreased, emphasising the transformation of C≡N groups to C = N [29]. Importantly, this reduction was more pronounced in the S6 sample spectrum, indicative of a more complete stabilisation process for this heating profile. Comparison of the spectra related to S4, S5, and S6 revealed that increasing the stabilisation duration from 22 to 28 min, appeared to lead to only a modestly weaker peak at 2240 cm^{-1} suggesting that while time of stabilisation remains important, temperature plays a more dominant role. This is reflected in Fig. 1c which exhibits a steady increase in the EOR with increasing temperature, from 71.3 % for the S1 sample to 79.6 % and 81.7 % for S3 and S6, respectively. The effect of increasing the dwell time from 22 min to 28 min for S4 and S6 samples, only increased the EOR from 80 % to 81.7 %.

Table 2
Enthalpy values and stabilisation yields of acrylic yarns after undergoing different heating profiles.

Samples	Control acrylic yarn	S1	S2	S3	S4	S5	S6
ΔH (J/g)	913	780	431	389	413	407	79
SY%	–	14.6	52.8	57.4	54.8	55.4	91.3

3.2. Thermal characteristics of the stabilised yarns

Fig. 2a and b show the DSC thermograms of the control and oxidised acrylic yarns as a function of temperature and residence time respectively. It is known that the thermal stabilisation process of acrylic fibres is an exothermic process [37,38]. Table 2 presents the exothermic enthalpy (ΔH) value and the calculated stabilisation yield for each of the oxidised yarns. The control sample exhibited a strong typical exothermic peak at 300 °C, which is again attributed to the dehydrogenation, cyclisation, and crosslinking reactions discussed above [29]. Although a less direct measurement of chemical change, the reduction and broadening of the enthalpy and the exothermic peak shifting to higher temperatures is clearly observed for the oxidised samples when compared with the control yarn [39]. Compared with FTIR, the DSC stabilisation yields displayed somewhat similar trends, such as increasing with increasing temperature, but the additional oxidation time for the S6 profile resulted in a much higher yield. The S1 sample exhibited the lowest stabilisation yield of only 14.6 %, but this increased to 52.7 % and 57.3 % as the temperatures increased through the different zones by 10–15 °C based on the S2 and S3 profiles, respectively. The biggest impact in stabilisation yield was observed for the S6 profile where the extension of oxidation time from 25 to 28 min led to near total disappearance of the exothermic peak, increasing the stabilisation yield to 91.3 %. As a result, longer oxidation times were deemed unnecessary due to the likely deleterious impact upon mechanical properties which would hamper weavability. These results highlighted the key roles of temperature and residence time factors in completing the transformation of linear structure to the ladder-like required for an oxidised acrylic fibre.

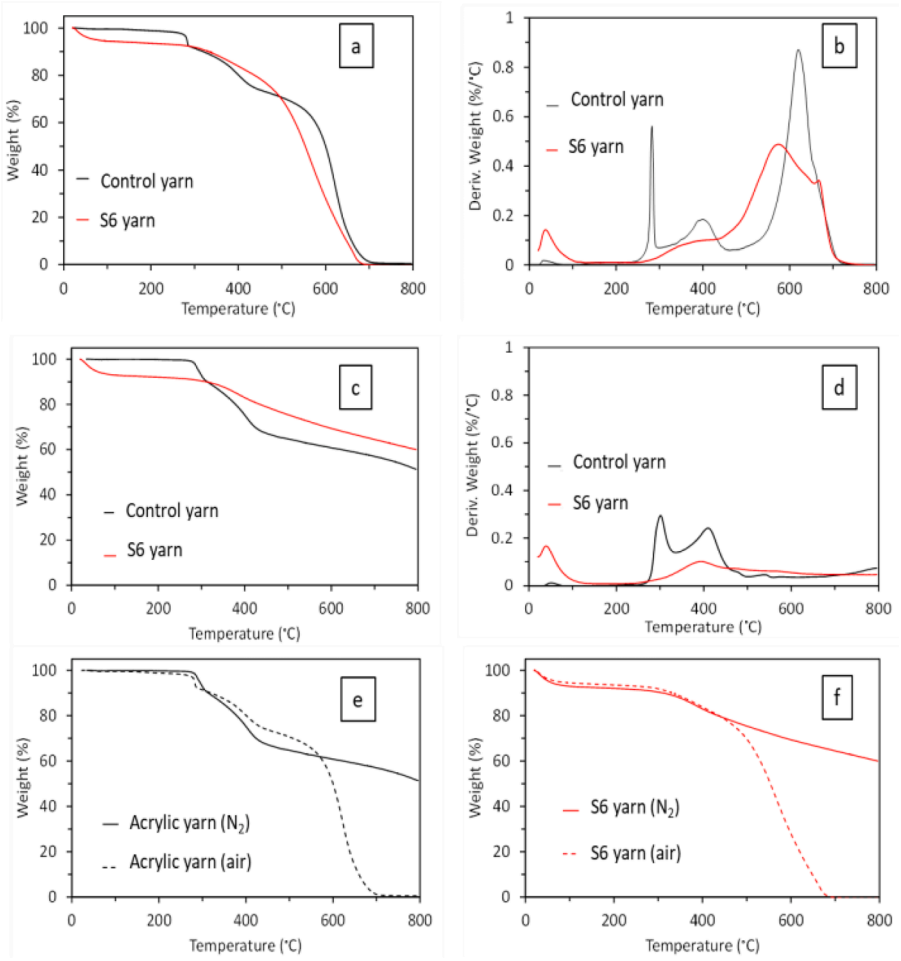

Fig. 3. (a) TGA and (b) DTG thermographs of control and oxidised S6 acrylic yarns under air, (c) TGA and (d) DTG thermographs of control and oxidised S6 acrylic yarns tested under N_2; and TGA thermographs of (e) control acrylic yarn, and (f) the S6 sample under nitrogen and air atmospheres.

Taking the sample exposed to the S6 profile, the most efficient profile for stabilisation, the TGA and DTG thermographs were compared to the control sample (Fig. 3). As can be seen, different decomposition trends under air and N_2 atmospheres are observed. The S6 stabilisation profile increased the onset of decomposition temperatures regardless of atmosphere and reduced the mass loss and rate of mass loss of the yarn. The control yarn tested in air showed three mass loss regions; at onset temperatures of 280, 362 and 583 °C, attributed to the (1) cyclisation reactions and the release of hydrogen cyanide and ammonia gases, (2) decomposition-carbonisation of the cyclic structure, and (3) oxidation and volatilisation of the formed char, respectively [5,40,41]. Based on the corresponding DTG curve, it was realised that the second decomposition region was not an intense reaction as the amount of the generated heat was much less than other two stages. In addition, the DTG graph of the S6 sample tested under air demonstrated that the most significant mass loss was related to the thermo-oxidation of the remaining char at temperatures >500 °C. No significant reactions were also detected for the zones related to cyclisation, and decomposition-carbonisation of the cyclic structures in the tested S6 sample.

By changing the atmosphere to nitrogen, the control yarn displayed much greater thermal stability up to 300 °C after which two distinctive decomposition regions were evident. As would be expected, the step related to the oxidation/volatilisation of the char was eliminated. The sample experienced a steady decomposition up to 800 °C and a char yield of 51 % was recorded (Fig. 3c). The corresponding DTG showed a significant reduction in peak intensities for these two decomposition regions (Fig. 3d). The S6 sample, although displaying an initial reduction in mass at low temperature, displayed a char yield of 60 % at 800 °C and a higher onset of decomposition. The corresponding DTG also displayed a much lower rate of mass loss affirming the greater thermal stability of S6 compared with the control yarn. Comparing the TGA thermograms of the control acrylic yarn under air and nitrogen showed that the presence of oxygen slightly improved the stability of the sample at temperatures <570 °C, while accelerated the oxidation of residues and weight loss in higher temperatures (Fig. 3e). These findings were consistent with Horrocks et al. [42]. For the S6 sample, the presence of oxygen did not have any effect on the weight loss trend of the yarn at temperatures below ~500 °C; however, it increased the weight loss then after, (i.e., temperatures > ~500 °C) (Fig. 3f). Table 3 compares the

Table 3
Thermal behaviour of control sample and oxidised S6 acrylic yarn based on their TGA and DTG traces.

Sample (Testing atmosphere)	T_{onset} (°C)	T_{max} (°C)	Mass loss (%)	Residue (%)
Control acrylic yarn (air)	280	283	100	0
	362	400		
	583	662		
Oxidised S6 (air)	318	-	100	0
	508	566		
Control acrylic yarn (N_2)	280	289	49	51
	373	405		
Oxidised S6 (N_2)	323	388	40	60

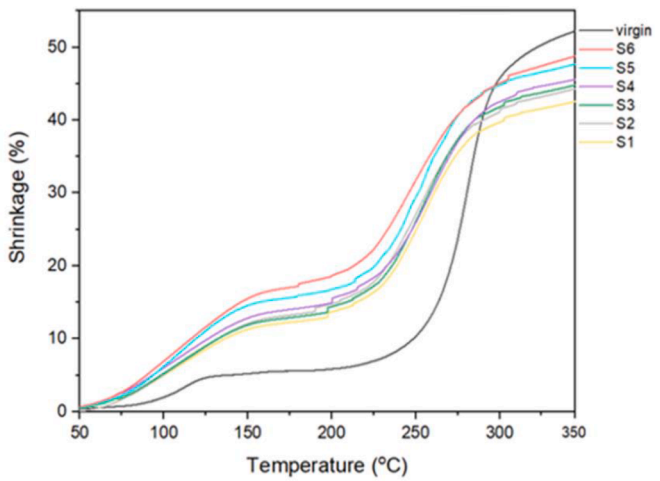

Fig. 4. Fibre shrinkage characteristics measured by DMA.

withstand the stresses imposed during continuous processing through an oxidation line. For this reason, DMA analysis was used in the creep mode to measure linear shrinkage of the control yarn and the oxidised samples. The results in Fig. 4 revealed two distinct transitions that can be attributed first to physical and, then to chemically induced shrinkage during stabilisation [43]. Physical shrinkage likely arises from the greater interactions between individual filaments while chemical shrinkage arises from the covalent bonding within the network replaces non-covalent bonds. The virgin yarn exhibits lower shrinkage initially in the first step, followed by much larger shrinkage as the chemically induced shrinkage begins to dominate. For the oxidised samples, overall shrinkage, increased from 44.4 % to 48.9 % for S1 and S6 fibres, respectively (Fig. 4).

3.3. Flammability of yarns

The purpose of this work is to reduce the flammability of acrylic yarns whilst maintaining processability. Images of the differences in combustion behaviour are shown in Fig. 5 and Videos S1-S7[1], which

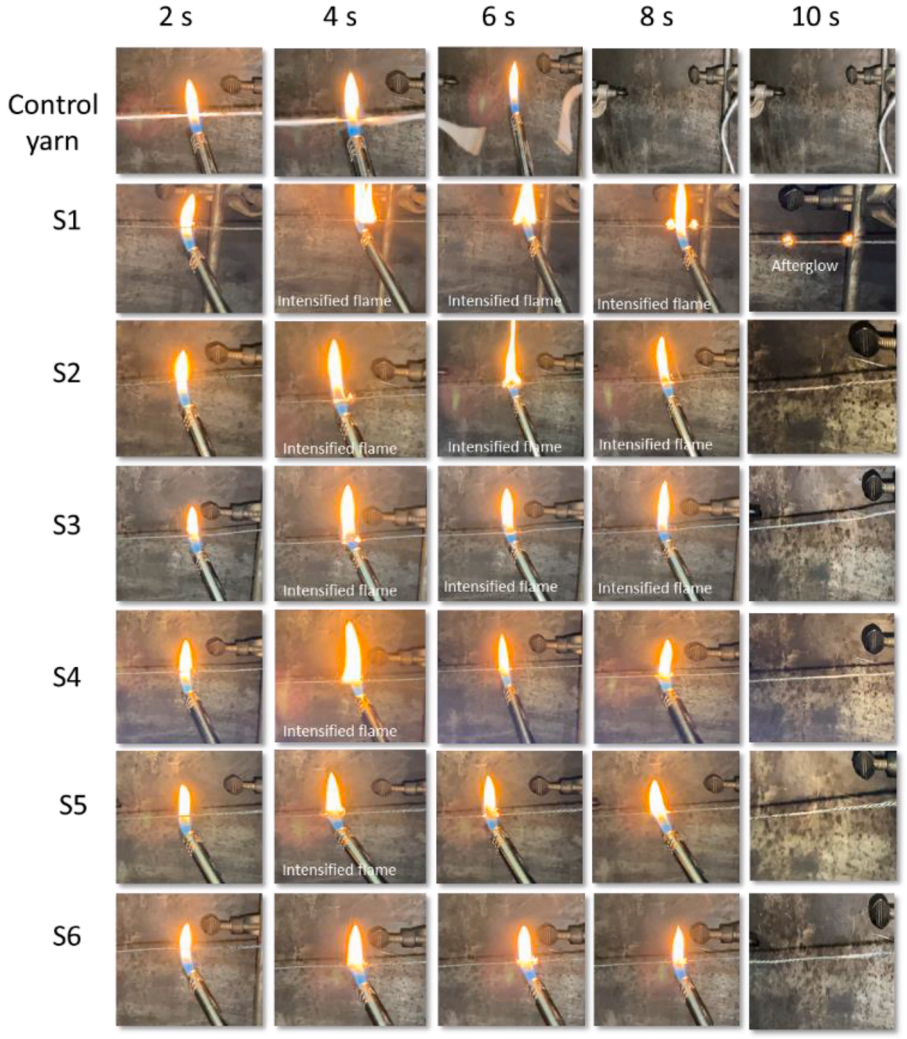

Fig. 5. Testing the flammability of control and oxidised acrylic yarns after 10 s in contact with flame.

thermal behaviours of S6 and control acrylic yarns based on their TGA and DTG thermographs.

The acrylic yarn is a commercially available twisted continuous fibre that undergoes shrinkage during heating. Therefore, the extent of shrinkage will play an important role in determining the fibre's ability to clearly illustrate the superior performance of the oxidised samples

[1] Video S1: Yarn S1, Video S2: Yarn S2, Video S3: Yarn S3, Video S4: Yarn S4, Video S5: Yarn S5, Video S6: Yarn S6, Video S7: Control acrylic yarn

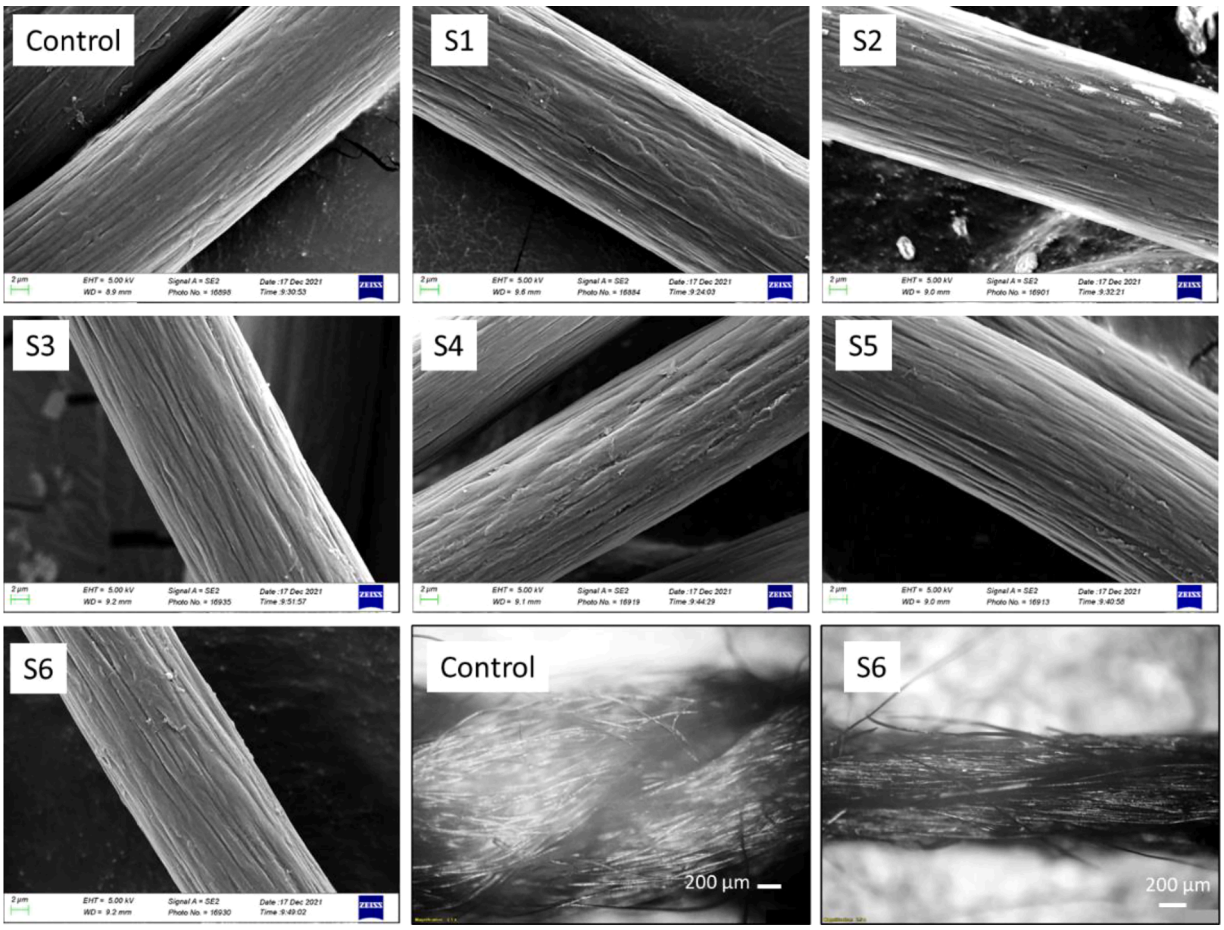

Fig. 6. SEM images of individual acrylic fibres before and after thermal stabilisation process, and optical microscopy images of control and S6 yarns (bottom-middle and bottom-right).

compared with the control yarn. Polyacrylonitrile is a synthetic polymer whose melting point is higher than its degradation temperature, but if heating is too rapid, the melting of fibres will still occur [4]. This phenomenon was observed during burning of the control yarn where it readily burnt, melted, and tore apart after exposure to the flame for only 6 s. The oxidised fibres were clearly more resistant to fire, with the S6 sample displaying the best performance. Exposing the S1 sample to fire for only 4 s ignited the yarn and the flame intensified. A weak self-extinguishing property was observed after the removal of the flame but burning continued along the length of the yarn. Important to note, the stabilisation yield for S1 was 14.6 %. Increasing the stabilisation temperature for the S2, and S3 profiles and residence times based on S4, S5, and S6 profiles both reduced the flammability of yarns and improved their self-extinguishing character. S2 (SY = 52.8 %) and S3 (SY = 57.4 %) samples were oxidised for 28 min but they still displayed an intensified flame after 4 s contact with the flame, implying that the tested yarns still did not acquire adequate fire retardancy. However, the ignited flame did not spread along the yarn and maintained a strong self-extinguishing property. The S6 sample (SY = 91.3 %), which was oxidised for 28 min, and at the higher temperature profile of 240–255–270–280 did not show any ignition, after contact with a flame nor did it glow at all after the removal of the flame. These observations were consistent with the DSC results confirming the superior stabilisation of the S6 sample.

3.4. Microscopy of fibres and yarns

Scanning electron microscopy (SEM) was used to examine the microstructure of the oxidised fibres. As can be seen in Fig. 6 grooved structures on the surface of fibres can be observed which primarily relate to the manufacturing process of fibres. The SEM images suggest however that the oxidised fibres have modestly rougher surface morphologies compared with the control sample, which increases with increasing temperature. The diameter of the non-oxidised fibre was 17.2 ± 0.3 μm which slightly decreased to 15.1 ± 0.3 μm after processing based on the S6 heating profile. The diameter variation of the yarn was also assessed, and it was noticed that the diameter of the acrylic yarn experienced a significant reduction where it reduced from around 2.00±0.04 mm to approximately 0.90±0.02 mm after undergoing the heat treatment based on S6 profile as shown by the optical images (Fig. 6). This can be related to the effect of heat on inducing shrinkage on fibres within yarn structure during the oxidation process while the two ends of the yarn were fixed. Each individual fibre underwent shrinkage and induced an untwisting behaviour in the yarn to get an extra length and movement freedom. This extra length prevented the breakage of the fibres during the stabilisation process. After shrinkage, each individual fibre repositioned and stretched almost alongside each other, because of which the diameter of the oxidised yarn was significantly less than that of the bulky control acrylic yarn. The observed physical shrinkage was suggested to be related to the entropic recovery of changes imposed on acrylic polymer chains orientation during the fibre spinning stage [4]. The shrinkage occurs due to the intermolecular crosslinking reactions taking place between neighbouring polymer chains [44].

3.5. Effect of oxidation process on mechanical characteristics

Given the importance of balancing fire retardancy with mechanical properties, the tensile properties of the oxidised S6, as the most fire-

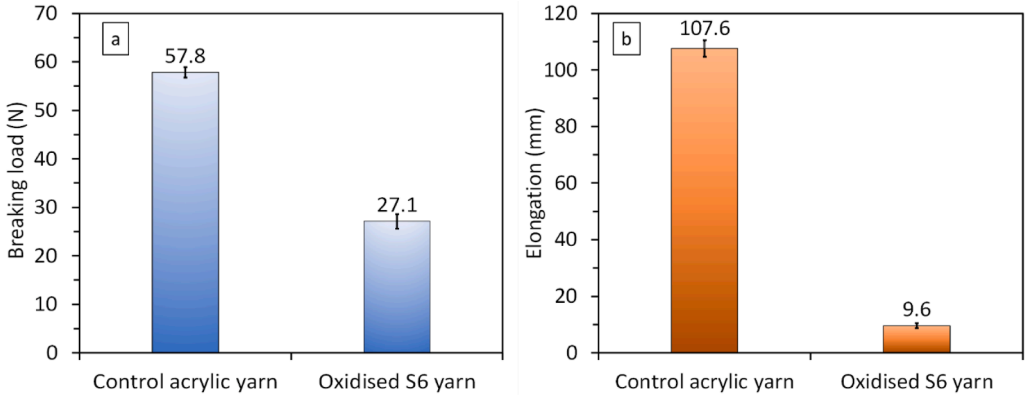

Fig. 7. Comparison of mechanical properties of S6 yarn with the control acrylic yarn (a) breaking load, and (b) elongation at break.

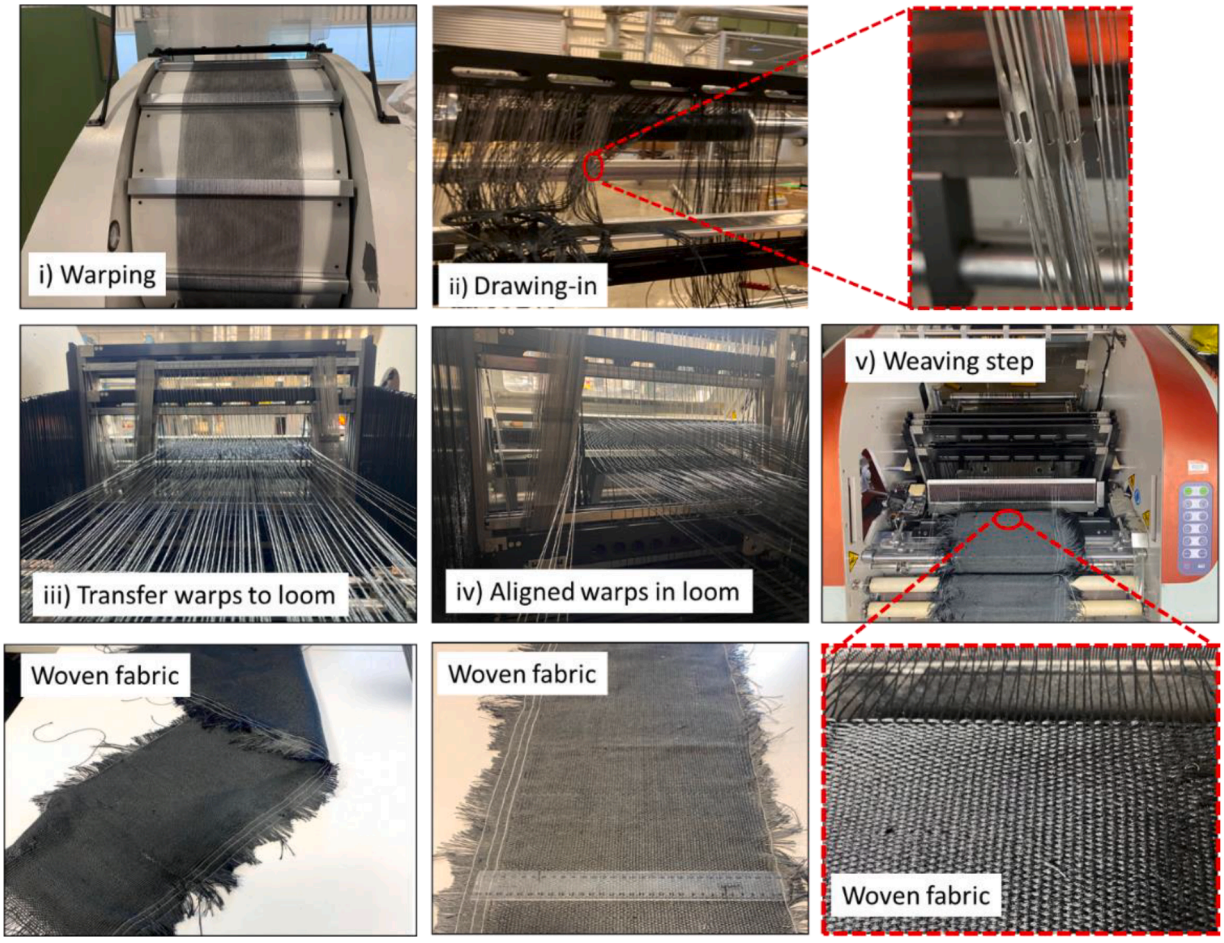

Fig. 8. Production process of woven fabric using oxidised S6 yarn.

retardant yarn, were compared with non-oxidised control sample (Fig. 7). The breaking load of the yarn decreased by around 53 % as a consequence of the stabilisation process which was due to forming weaker cross-links such as C = N groups in the oxidised fibres compared with acrylic fibres which contained C≡N [44]. This transformation lowered the cohesive force between the polymer chains appearing as lowered tensile properties and elasticity [44]. The elongation of the yarn decreased by 91 % after the stabilisation process and showed the transformation of a texturised flexible acrylic yarn into a more brittle one. It is important to note however, that despite the reduction in breaking load and elongation, the fibre remained strong enough to pass through multiple oxidation ovens during a continuous process withstanding the loads imparted by multiple free-wheeling metal rollers.

3.6. *Weavability of the oxidised yarn*

The weavability of the yarn produced using the S6 temperature profile was evaluated by weaving a plain weave fabric (Fig. 8). The important result from this weaving trial was to confirm that the non-combustible S6 yarn still possessed sufficient mechanical strength to withstand the applied tensions at different stages of the weaving process including warping, beaming, drawing-in, shedding, rapier weft picking,

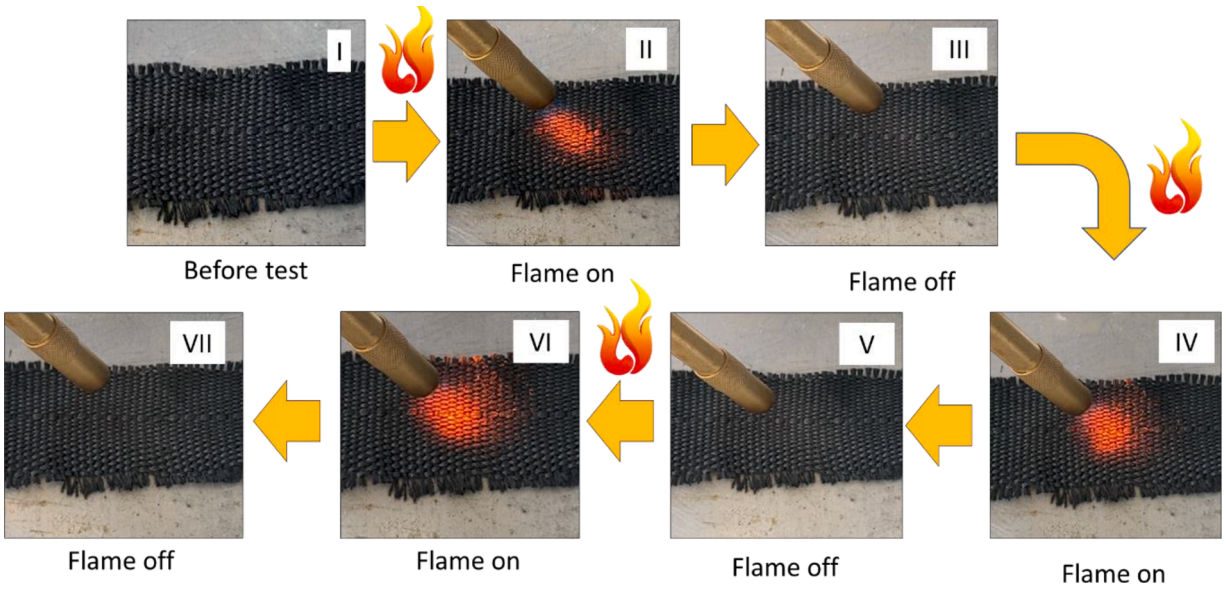

Fig. 9. Testing the fire retardancy of the woven fabric made of oxidised S6 yarn.

reed beating, and taking-up. Fire testing the woven fabric demonstrated its superior fire retardancy as shown in Videos S8 and S9. After three cycles of direct exposure to the propane gas flame, the woven structure of the fabric remained well preserved, and there was no sign of yarn damage at all. During exposure to the flame, the surface of the fabric glowed brightly but immediately dissipated after elimination of flame (Fig. 9). Importantly, there was no sign of burning nor after-glow on the tested fabric further supporting the non-combustible nature of this fabric. It was noticed that even after conducting a cyclic flame test, the fabric was still flexible and no breakages in the yarns were observed (Video S10). In the woven structure of fabric, all yarns showed an excellent fire retardancy which can corroborate the uniformity and consistency of the obtained fire-retardancy in the length of yarns.

4. Conclusion

A commercially available low-cost acrylic yarn has been subjected to a thermal stabilisation process to impart an optimum balance of superior fire retardancy and adequate mechanical properties suitable for weaving. The effects of the stabilisation temperature and time on the chemical, thermal, and mechanical characteristics of acrylic yarns were discussed. It was demonstrated that the typical exothermic peak of the acrylic yarn after oxidation at 240–255–270–280 °C with 28 min dwell time disappeared, indicating high levels of cyclisation in the processed yarn. This structural transformation imparted excellent fire retardancy to the oxidised sample (S6), while the samples prepared at lower temperatures and durations did not match this performance. In addition, TGA analysis demonstrated the high thermal stability of the oxidised yarn processed based on the mentioned heating profile, up to 800 °C. Testing the weavability of the oxidised yarn confirmed that they have the required mechanical strength to withstand the tensions of different stages of the weaving process. These results can pave the way for further application of fire-retardant acrylic-based fibres for daily life and technical areas. This method obviates the need to use high concentrations of hazardous chemicals and additives to create effective fire-retardant acrylic-based products.

CRediT authorship contribution statement

Esfandiar Pakdel: Conceptualization, Methodology, Investigation, Writing – original draft, Data curation. **Masihullah Jabarulla Khan:** Conceptualization, Methodology, Investigation. **Nguyen Le Thao Nguyen:** Investigation. **Maxime Maghe:** Investigation. **Russell J. Varley:** Conceptualization, Supervision, Resources, Writing – review & editing.

Declaration of Competing Interest

The authors declare the following financial interests/personal relationships which may be considered as potential competing interests:

Esfandiar Pakdel reports financial support was provided by Deakin University. no conflicts of interest to declare.

Data availability

Data will be made available on request.

Acknowledgement

The authors acknowledge Deakin's Advanced Characterisation Facility and the Australian National Fabrication Facility (ANFF) Victorian node at Deakin University. Partial Funding for this project was obtained from the Australian Federal Government funded Innovative Manufacturing Co-operative Research Centre, (IM-CRC) under the Activate Program. This project was also strongly supported by Gale-Pacific Pty Ltd and the authors would particularly like to thank Mr Andrew Nasarczyk and Mr Tony Grigoriadis for their collaboration and support.

Supplementary materials

Supplementary material associated with this article can be found, in the online version, at doi:10.1016/j.polymdegradstab.2023.110571.

References

[1] H. liu, L. Shi, P. Han, S. Ullah, J. Yu, B. Yang, C. Li, C. Zhu, J. Xu, Hierarchically porous carbon derived from waste acrylic fibers for super-high capacity lithium ion battery anodes, Chem. Eng. J. 346 (2018) 143–150.

[2] M.K. Singh, A. Singh, Fibers and fiber-forming polymers, in: M.K. Singh, A. Singh (Eds.), Characterization of Polymers and Fibres, Woodhead Publishing, Duxford, 2022, pp. 1–27.

[3] P. Bajaj, A.K. Agrawal, A. Dhand, N. Kasturia, Hansraj, Flame retardation of acrylic fibers: an overview, J. Macromol. Sci. Part C 40 (2000) 309–337.

[4] B.G. Frushour, R.S. Knorr, Acrylic fibers, in: M. Lewin (Ed.), Handbook of Fiber Chemistry, Taylor and Francis Group, LLC, London, 2007.
[5] R. Horrocks, J. Hicks, P. Davies, A. Alderson, J. Taylor, Synergistic flame retardant copolymeric polyacrylonitrile fibres containing dispersed phyllosilicate clays and ammonium phosphate, in: T.R. Hull, B.K. Kandola (Eds.), Fire Retardancy of Polymers, Royal Society of Chemistry, Cambridge, 2009, pp. 307–330.
[6] C.K. Kundu, Z. Li, L. Song, Y. Hu, An overview of fire retardant treatments for synthetic textiles: from traditional approaches to recent applications, Eur. Polym. J. 137 (2020), 109911.
[7] J.S. Tsai, The effect of flame-retardants on the properties of acrylic and modacrylic fibres, J. Mater. Sci. 28 (1993) 1161–1167.
[8] A.R. Horrocks, Textile flammability research since 1980 – personal challenges and partial solutions, Polym. Degrad. Stab. 98 (2013) 2813–2824.
[9] X. Yan, W. Zhou, X. Zhao, J. Xu, P. Liu, Preparation, flame retardancy and thermal degradation behaviors of polyacrylonitrile fibers modified with diethylenetriamine and zinc ions, J. Therm. Anal. Calorim. 124 (2016) 719–728.
[10] E. Pakdel, J. Fang, L. Sun, X. Wang, Nanocoatings for smart textiles, in: N.D. Yilmaz (Ed.), Smart Textiles: Wearable Nanotechnology, Wiley, 2018, pp. 247–300. https://doi.org/10.1002/9781119460367.ch8.
[11] M.P. Gashti, E. Pakdel, F. Alimohammadi, Nanotechnology-based coating techniques for smart textiles, in: J. Hu (Ed.), Active Coatings for Smart Textiles, Woodhead Publishing, Duxford, 2016, pp. 243–268. https://doi.org/10.1016/B978-0-08-100263-6.00011-3.
[12] M.J. Tsafack, J. Levalois-Grützmacher, Plasma-induced graft-polymerization of flame retardant monomers onto PAN fabrics, Surf. Coat. Technol. 200 (2006) 3503–3510.
[13] Y. Ren, Y. Gu, Q. Zeng, Y. Zhang, UV-induced surface grafting polymerization for preparing phosphorus-containing flame retardant polyacrylonitrile fabric, Eur. Polym. J. 94 (2017) 1–10.
[14] Y. Ren, T. Tian, L. Jiang, X. Liu, Z. Han, Polyvinyl alcohol reinforced flame-retardant polyacrylonitrile composite fiber prepared by boric acid cross-linking and phosphorylation, Materials 11 (2018) 2391.
[15] J.Z. Xu, C.M. Tian, Z.G. Ma, M. Gao, H.Z. Guo, Z.H. Yao, Study on the thermal behaviour and flammability of the modified polyacrylonitrile fibers, J. Therm. Anal. Calorim. 63 (2000) 501–506.
[16] W. Zhou, X. Yan, P. Liu, M. Jiang, J. Xu, Flame retardant modification of acrylic fiber with hydrazine hydrate and sodium ions, J. Appl. Polym. Sci. 132 (2015) 41996.
[17] F. Carosio, J. Alongi, Flame retardant multilayered coatings on acrylic fabrics prepared by one-step deposition of chitosan/montmorillonite complexes, Fibers 6 (2018) 36.
[18] T. Groetsch, M. Maghe, C. Creighton, R.J. Varley, Environmental, property and cost impact analysis of carbon fibre at increasing rates of production, J. Clean. Prod. 382 (2023), 135292.
[19] Q. Wang, W. Bai, X. Lu, J. Wang, E. Pakdel, Z. Yu, Y. Cui, Q. Liu, Thermally oxidized PAN as photocatalyst support layer for VOCs removal, J. Text. Inst. (2023), https://doi.org/10.1080/00405000.2023.2240058.
[20] E. Pakdel, S. Kashi, R. Varley, X. Wang, Recent progress in recycling carbon fibre reinforced composites and dry carbon fibre wastes, Resour. Conserv. Recycl. 166 (2021), 105340.
[21] H.S. Kil, S. Lee, High flame retardancy of oxidized polyacrylonitrile fibers prepared by effective plasma-assisted thermal stabilization and electron-beam irradiation, Compos. Part B Eng. 178 (2019), 107458.
[22] B.S. Gupta, M. Afshari, Polyacrylonitrile fibers, in: A.R. Bunsell (Ed.), Handbook of Properties of Textile and Technical Fibres, Woodhead Publishing, Duxford, 2018, pp. 545–593.
[23] U. Sayed, H. Jain, S. Raghupathy, Oxidised polyacrylonitrile fibre as a flame retardant material, Int. J. Adva. Sci. Eng. 2 (2016) 155–158.
[24] E. Ismar, A.S. Sarac, Nonflammable pre-carbonized polyacrylonitrile nanofiber webs, SN Appl. Sci. 2 (2020) 589.
[25] B.N.S. Rafiei, S. Arbab, A.K. Haghi, Stabilization process of PAN nanofibers, in: R. A. Pethrick, E.M. Pearce, G.E. Zaikov (Eds.), Polymer Products and Chemical Processes, Apple Academic Press, New York, 2013, pp. 125–138.
[26] C. Zhang, R. Li, J. Liu, S. Guo, L. Xu, S. Xiao, Z. Shen, Hydrogen peroxide modified polyacrylonitrile-based fibers and oxidative stabilization under microwave and conventional heating – the 1st comparative study, Ceram. Int. 45 (2019) 13385–13392.
[27] H. Khayyam, R.N. Jazar, S. Nunna, G. Golkarnarenji, K. Badii, S.M. Fakhrhoseini, S. Kumar, M. Naebe, PAN precursor fabrication, applications and thermal stabilization process in carbon fiber production: experimental and mathematical modelling, Prog. Mater. Sci. 107 (2020), 100575.
[28] K.Ş. Tunçel, M.M. Rahman, T. Demirel, I. Karacan, The impact of guanidine carbonate incorporation on the molecular structure of polyacrylonitrile precursor fiber stabilized by a multistep heat treatment strategy, Polym. Eng. Sci. 62 (2022) 1081–1095.
[29] Q. Duan, B. Wang, H. Wang, Effects of stabilization temperature on structures and properties of polyacrylonitrile (PAN)-based stabilized electrospun nanofiber mats, J. Macromol. Sci. Part B 51 (2012) 2428–2437.
[30] Z. Fu, Y. Gui, C. Cao, B. Liu, C. Zhou, H. Zhang, Structure evolution and mechanism of polyacrylonitrile and related copolymers during the stabilization, J. Mater. Sci. 49 (2014) 2864–2874.
[31] Y. Liu, Y. Xue, H. Ji, J. Liu, Kinetics of the cyclization and isomerization reactions in polyacrylonitrile based carbon fiber precursors during thermal-oxidative stabilization, J. Appl. Polym. Sci. 137 (2020) 48819.
[32] J. Zhao, J. Wang, L. Fan, E. Pakdel, S. Huang, X. Wang, Immobilization of titanium dioxide on PAN fiber as a recyclable photocatalyst via co-dispersion solvent dip coating, Text. Res. J. 87 (2017) 570–581.
[33] H. Liu, S. Zhang, J. Yang, M. Ji, J. Yu, M. Wang, X. Chai, B. Yang, C. Zhu, J. Xu, Preparation, stabilization and carbonization of a novel polyacrylonitrile-based carbon fiber precursor, Polymers 11 (2019) 1150.
[34] H. Kakida, K. Tashiro, M. Kobayashi, Mechanism and kinetics of stabilization reaction of polyacrylonitrile and related copolymers I. Relationship between isothermal DSC thermogram and FT/IR spectral change of an acrylonitrile/methacrylic acid copolymer, Polym. J. 28 (1996) 30–34.
[35] I. Shimada, T. Takahagi, M. Fukuhara, K. Morita, A. Ishitani, FT-IR study of the stabilization reaction of polyacrylonitrile in the production of carbon fibers, J. Polym. Sci. Part A Polym. Chem. 24 (1986) 1989–1995.
[36] M. Guo, X. Qian, J. Zhong, C. Li, H. Gong, Y. Zhang, Modification of large tow textile grade polyacrylonitrile fiber by dopamine hydrochloride to prepare low-cost carbon fibers, Polym. Degrad. Stab. 211 (2023), 110332.
[37] X. Jin, C. Feng, C. Creighton, N. Hameed, J. Parameswaranpillai, N.V. Salim, On the structural evolution of textile grade polyacrylonitrile fibers during stabilization and carbonization: towards the manufacture of low-cost carbon fiber, Polym. Degrad. Stab. 186 (2021), 109536.
[38] M. Jing, C.G. Wang, Q. Wang, Y.J. Bai, B. Zhu, Chemical structure evolution and mechanism during pre-carbonization of PAN-based stabilized fiber in the temperature range of 350–600°C, Polym. Degrad. Stab. 92 (2007) 1737–1742.
[39] W. Dang, J. Liu, X. Wang, K. Yan, A. Zhang, J. Yang, L. Chen, J. Liang, Structural transformation of polyacrylonitrile (PAN) fibers during rapid thermal pretreatment in nitrogen atmosphere, Polymers 12 (2020) 63.
[40] C. Zuo, X. Su, Y. Guo, Y. Ren, X. Liu, Fabrication of halogen-free and phosphorus-free flame retardant and antistatic PAN fibers based on tea polyphenol phenolic resin chelated with iron (III) ions, Polym. Degrad. Stab. 214 (2023), 110384.
[41] Y. Guo, C. Zuo, W. Tan, Y. Liu, L. Jiang, D. Yu, Y. Ren, X. Liu, Fabricating flame retardant polyacrylonitrile fibers modified by sodium lignosulfonate and copper ions, Polym. Degrad. Stab. 206 (2022), 110176.
[42] A.R. Horrocks, J. Zhang, M.E. Hall, Flammability of polyacrylonitrile and its copolymers II. Thermal behaviour and mechanism of degradation, Polym. Int. 33 (1994) 303–314.
[43] E. Fitzer, W. Frohs, M. Heine, Optimization of the processes of stabilization (oxidation) and carbonization of PAN fibres and structural characteristics which define the properties of carbon fibres, Carbon 24 (1986) 387.
[44] L.M. Manocha, O.P. Bahl, Role of oxygen during thermal stabilisation of pan fibres, Fibre Sci. Technol. 13 (1980) 199–212.